

# AUS Repository

## Indoor Source Apportionment and Health Risk Assessment of Inorganic PM<sub>2.5</sub> in a University Building in the UAE

Item Type	Article;Published version;Peer-Reviewed
Authors	Anwar, Shahid;Satheesh, Vipin;Shameer, Mohamed;Alawadhi, Hussain;Hamdan, Nasser M.
Citation	Anwar, S., Satheesh, V., Shameer, M., Alawadhi, H., & Hamdan, N. M. (2026). Indoor Source Apportionment and Health Risk Assessment of Inorganic PM <sub>2.5</sub> in a University Building in the UAE. <i>Indoor Air</i> , 2026(1). <a href="https://doi.org/10.1155/ina/2235690">https://doi.org/10.1155/ina/2235690</a>
DOI	<a href="https://doi.org/10.1155/ina/2235690">10.1155/ina/2235690</a>
Publisher	Wiley
Rights	Attribution 4.0 International
Download date	2026-06-08 18:59:25
Item License	<a href="http://creativecommons.org/licenses/by/4.0/">http://creativecommons.org/licenses/by/4.0/</a>
Link to Item	<a href="https://hdl.handle.net/11073/33436">https://hdl.handle.net/11073/33436</a>

## RESEARCH ARTICLE OPEN ACCESS

# Indoor Source Apportionment and Health Risk Assessment of Inorganic PM<sub>2.5</sub> in a University Building in the UAE

Shahid Anwar<sup>1</sup> | Vipin Satheesh<sup>2</sup> | Mohamed Shameer<sup>3</sup> | Hussain Alawadhi<sup>3</sup> | Nasser M. Hamdan<sup>1,2,3</sup>

<sup>1</sup>Materials Science and Engineering Program, College of Arts and Sciences, The American University of Sharjah, Sharjah, UAE | <sup>2</sup>Physics Department, The American University of Sharjah, Sharjah, UAE | <sup>3</sup>Center for Advanced Materials Research, Research Institute of Sciences and Engineering, University of Sharjah, Sharjah, UAE

**Correspondence:** Nasser M. Hamdan (nhamdan@aus.edu)

**Received:** 1 July 2025 | **Revised:** 29 March 2026 | **Accepted:** 8 April 2026

**Academic Editor:** Parthipan Punniyakotti

**Keywords:** hazard quotient | health risk assessment | indoor air quality | Multiple-Path Particle Dosimetry | PM<sub>2.5</sub> | PMF | source apportionment

## ABSTRACT

Indoor air quality (IAQ) is a growing public health concern, especially in environments where individuals spend the majority of their time, such as homes, educational institutions, and office environments. This study investigates the elemental composition, chemical speciation, source apportionment, and health risks associated with indoor PM<sub>2.5</sub> in a university building in the United Arab Emirates over a 1-year period. An indoor sampling campaign was conducted following international standards, and elemental analysis was performed using energy-dispersive X-ray fluorescence (EDXRF) spectroscopy. Crystallographic phases and compound identification were performed using X-ray diffraction (XRD) and scanning electron microscopy with energy-dispersive X-ray spectroscopy (SEM/EDS), respectively. Positive Matrix Factorization (PMF v5.0) was applied to apportion pollution sources, while health risk assessments were conducted for trace element exposure based on methods from the US EPA and the Agency for Toxic Substances and Disease Registry (ATSDR). Key indoor PM<sub>2.5</sub> contributors included mineral and resuspended dust, sea salt, and anthropogenic sources such as heavy oil combustion, traffic, and secondary aerosols. The health risk assessment showed that all analyzed elements (Cr, Mn, Al, As, Cu, Ni, Pb, Zn, and Mg) had hazard quotient values below 1, indicating no noncarcinogenic risk, and the carcinogenic risk values for As, Cr, Ni, and Pb were below the ATSDR's threshold value of  $1 \times 10^{-6}$ . Multiple-Path Particle Dosimetry modeling showed that approximately 75% of inhaled PM<sub>2.5</sub> deposits in the respiratory system, with younger individuals (18 years old) exhibiting slightly lower deposition. After 5 days of exposure, alveolar retention reached 0.072 mg in 21-year-olds and 0.066 mg in 18-year-olds, indicating potential for prolonged internal deposition. The findings underscore the importance of continuous monitoring and mitigation strategies to improve IAQ in densely occupied indoor environments.

## 1 | Introduction

Indoor air quality (IAQ) has become a major public health concern because most people spend nearly 90% of their time indoors, in homes, workplaces, public buildings, or while commuting, and are therefore exposed to indoor and infiltrated outdoor pollutants [1, 2].

Among these pollutants, particulate matter (PM) with an aerodynamic diameter of  $\leq 2.5 \mu\text{m}$  (PM<sub>2.5</sub>) is of particular concern due to its ability to penetrate deep into the respiratory system. Numerous epidemiological studies have linked both short- and long-term PM<sub>2.5</sub> exposure to adverse health effects, including cardiovascular diseases, chronic obstructive pulmonary disease (COPD), asthma, and premature mortality [3, 4]. COPD is

This is an open access article under the terms of the [Creative Commons Attribution](https://creativecommons.org/licenses/by/4.0/) License, which permits use, distribution and reproduction in any medium, provided the original work is properly cited.

Copyright © 2026 Shahid Anwar et al. *Indoor Air* published by John Wiley & Sons Ltd.





**FIGURE 1** | Location of the sampling site. The main panel shows the position of the American University of Sharjah on the southern coast of the Arabian Gulf, with a zoomed inset highlighting the urban area surrounding the campus where the indoor  $PM_{2.5}$  measurements were conducted. Base map: Google Earth.

lower detection limit (LDL) values are shown in Supporting Information 1: Table S1. Calibration accuracy and data reliability were validated by analyzing the NIST standard reference material SRM 2783 using the same protocol as for the Micromatter standards. Quantification of elemental mass per area ( $\mu\text{g cm}^{-2}$ ) was converted into volumetric concentrations ( $\mu\text{g m}^{-3}$ ) based on gravimetric  $PM_{2.5}$  mass, allowing the determination of the relative abundance of each detected element. The results for SRM 2783 showed strong agreement with certified NIST values [26].

Morphological analysis of selected samples was conducted using SEM with a TESCAN VEGA3 XMU system. Elemental mapping was performed using EDS (Oxford Aztec X-Max 50) integrated with SEM. Additionally, XRD analysis was carried out using a Bruker D8 ADVANCE instrument to identify mineral phases present in selected filter samples.

### 2.3 | Elemental Black Carbon (eBC) Analysis

eBC concentration was determined using the EEL Model 43M Smokestain Reflectometer, which quantifies the optical darkness of particulate deposits collected on Teflon filter media [27]. The analysis was performed on the  $PM_{2.5}$ -loaded Teflon filters after gravimetric weighing. Each filter was analyzed by placing the filter directly onto the reflectometer stage. The reflectance ( $R$ ) was measured at two distinct locations on the filter surface to account for possible loading inhomogeneity, and the average value was used to calculate the eBC concentration. Prior to analysis, the filters were preconditioned under controlled laboratory conditions at  $20 \pm 1^\circ\text{C}$  temperature and  $50 \pm 5\%$  relative humidity. The instrument was calibrated using blank filters and internal calibration factors.

The  $R$  is inversely proportional to black carbon concentration. The attenuation of light is related to the eBC mass using Equation (1):

$$\text{eBC} \left( \frac{\mu\text{g}}{\text{m}^3} \right) = \frac{A \times 10^6}{2V \times \sigma_{\text{ATN}}} \cdot \ln \left( \frac{R_0}{R} \right) \left( 1 + k \cdot \ln \left( \frac{R_0}{R} \right) \right), \quad (1)$$

where

- $R_0$ : reflectance of a blank filter.
- $R$ : reflectance of the sampled filter.
- $A$ : area of the exposed part of a filter ( $12.9 \text{ cm}^2$ ).
- $\sigma_{\text{ATN}}$ : mass extinction coefficient ( $19.5 \text{ m}^2 \text{ g}^{-1}$ ) for a Teflon filter.
- $V$ : volume of air sampled.
- $k$ : shadowing correction factor (0.3).

This optical method provides a rapid, nondestructive estimate of black carbon mass based on its light-absorbing properties [28].

### 2.4 | Source Apportionment

The source apportionment of indoor  $PM_{2.5}$  was performed using the United States Environmental Protection Agency's (US EPA) Positive Matrix Factorization (PMF) model v5.0, which separates a dataset into factor contributions and profiles [29, 30]. Variables with high uncertainty or low signal-to-noise (S/N) ratios were either downweighted or excluded to minimize model noise. Uncertainties were calculated by combining sampling, calibration, instrumentation, and analytical errors [31, 32]. For PMF analysis, two input matrices, the

concentration and uncertainty matrices, were prepared. An observation-based uncertainty file was used as input for the PMF model [33]. The uncertainty values are very critical in the PMF, and hence, we considered many parameters to calculate the uncertainty. For the instrument, the uncertainty was the standard deviation in the peak area given by the operating software. The calibration error was taken as 5%, which was taken from the Micromatter standards. Manual error while handling the samples in the field, transportation, weighing, and storage was taken as 15%. Finally, an error due to the attenuation of characteristic X-rays from light elements was considered. The total uncertainty was calculated as the square root of the sum of the squares of these uncertainties. Missing values were coded as -999, allowing the model to replace them with the species median. Elements with a high percentage of values below detection limits or zeros were flagged as “bad” variables in the PMF input. This preprocessing ensured that only statistically meaningful species contributed to the factor profiles. The model’s performance was assessed using goodness-of-fit indicators such as  $Q(\text{true})$ ,  $Q(\text{robust})$ , and  $Q/Q_{\text{exp}}$ , with consistent  $Q(\text{robust})$  values indicating reliable solutions [33, 34]. Factor numbers were finalized based on  $Q$ -value convergence, acceptable scaled residuals (-3 to +3), and interpretability of source profiles against known emission characteristics [35, 36]. Displacement (DISP) and Bootstrap (BS) runs were performed to further evaluate solution stability.

## 2.5 | Wind Rose Analysis

To evaluate regional wind dynamics during the study period, wind rose analysis was performed using the openair package in R. The meteorological data for the study duration were obtained from the National Aeronautics and Space Administration (NASA) Langley Research Center’s (LaRC) POWER Project, an initiative supported by the NASA Earth Applied Science Program [37]. The parameters included hourly wind speed (m/s) and wind direction ( $^{\circ}$ ) at 10-m altitude obtained from the MERRA-2 satellite.

## 2.6 | Health Risk Analysis

To assess potential health risks from airborne trace elements, both noncancer and cancer risks (CRs) were estimated using the standard risk assessment approach [38]. The hazard quotient (HQ) was calculated using Equation (2) to evaluate noncarcinogenic effects by comparing the exposure factor (EF)-adjusted air concentration (AAC) of each metal with its corresponding health guideline value [39].

$$\text{HQ} = \frac{\text{AAC}}{\text{RfC}}. \quad (2)$$

Here, AAC is the exposure concentration adjusted for exposure frequency and duration (in  $\mu\text{g}/\text{m}^3$ ), and RfC is the EPA’s reference concentration (in  $\mu\text{g}/\text{m}^3$ ) (Supporting Information 1: Table S1). An  $\text{HQ} > 1$  suggests potential for adverse noncancer effects.

For carcinogenic risk assessment, CR was calculated using Equation (3) [39]. The inhalation unit risk (IUR) values are provided by the US EPA and the State of California Office of Environmental Health Hazard Assessment (OEHHA) [40].

$$\text{CR} = \text{AAC} \times \text{IUR} \times \left( \frac{\text{ED}}{\text{LY}} \right). \quad (3)$$

Here, IUR is the inhalation unit risk ( $(\mu\text{g}/\text{m}^3)^{-1}$ ) (Supporting Information 1: Table S2), ED is the exposure duration (in years), and LY is the lifetime (male, 77.2 years old; female, 80.0 years old) [41]. A  $\text{CR} > 1.0 \times 10^{-6}$  indicates potential carcinogenic risk and warrants further toxicological evaluation. This methodology allows for screening and prioritizing pollutants for detailed health impact assessments.

Equation (4) is used to calculate EF-AACs, which modify measured air pollutant concentrations to reflect exposure frequency, duration, and time [39].

$$\text{AAC} = C_{\text{air}} \times \text{ET} \times \left( \frac{1 \text{ day}}{24 \text{ h}} \right) \times \text{EF}. \quad (4)$$

Here,  $C_{\text{air}}$  is the contaminant concentration in air ( $\mu\text{g}/\text{m}^3$ ), and ET is the exposure time (hours/day).

The EF is the exposure factor, calculated using the following equation [39]:

$$\text{EF} = \frac{F \times \text{ED}}{\text{AT}}, \quad (5)$$

with  $F$  as the exposure frequency (days/year) and AT as the averaging time (days).

## 2.7 | Deposition Analysis

The Multiple-Path Particle Dosimetry (MPPD) model is a mechanistic tool designed to estimate deposition and clearance of aerosols ranging from 1 nm to  $100 \mu\text{m}$  in human and animal respiratory systems [42, 43]. Version 3.04 of the MPPD model (Applied Research Associates, Inc.) (<https://www.ara.com/mppd/>), developed by the Hamner Institute for Health Sciences and the Dutch National Institute for Public Health and the Environment [44], was used to simulate  $\text{PM}_{2.5}$  behavior in occupants’ lungs using a 1-year average  $\text{PM}_{2.5}$  concentration of  $14.94 \mu\text{g}/\text{m}^3$  (input as  $0.01494 \text{ mg}/\text{m}^3$ ) [45]. Deposition, retention, and clearance simulations were set for 8 h/day, 5 days/week, over 1 week. Figure 2 shows the parameters used in the MPPD model.

## 3 | Results and Discussions

### 3.1 | Elemental Analysis and Chemical Speciation

In total, 94 samples were collected and analyzed over the 1-year campaign. A summary of  $\text{PM}_{2.5}$  concentrations and its major constituent elements, including eBC, Na, Mg, Al, Si, P, S, Cl, K, Ca, Ti, V, Cr, Mn, Fe, Ni, Cu, Zn, Br, Sr, Ba, and Pb, is given in Table 1, providing an overview of the IAQ in the study environment. The detailed elemental concentrations and their corresponding uncertainties are presented in Supporting Information 2 (Excel file EX1). Supporting Information 1: Table S4 contains a summary of the concentration of rarely

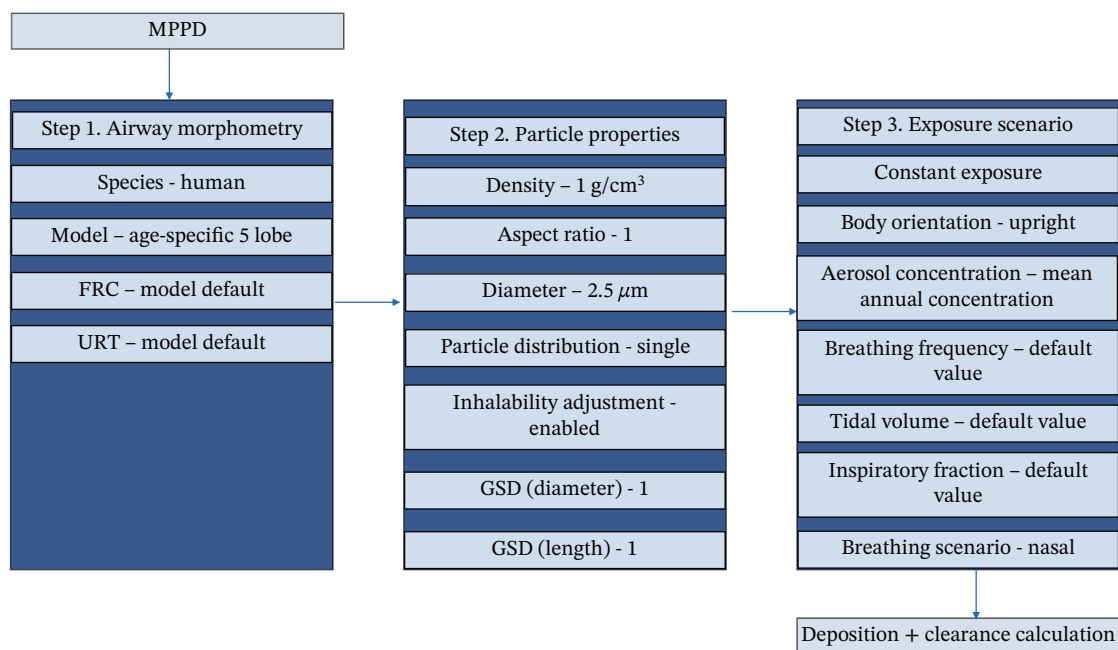


**FIGURE 2** | Parameters used in the MPPD model.

detected elements (Ga, As, Zr, and Rb). The annual average concentration of  $PM_{2.5}$  was found to be  $14.9 \mu\text{g}/\text{m}^3$ . The mean  $PM_{2.5}$  concentration during the warm/summer season (May–October) was  $15.3 \mu\text{g}/\text{m}^3$ , while during the cool/winter season (November–April), it was  $14.6 \mu\text{g}/\text{m}^3$ , indicating only a marginal difference between the two periods. This contrasts with the pronounced seasonal variation observed at a nearby outdoor monitoring site, where significantly elevated  $PM_{2.5}$  levels are typically recorded during the summer months [24]. However, this variation is not distinctly reflected in the indoor environment of the academic building under study. A likely explanation is the reduced building occupancy and minimal indoor activity during peak summer (particularly July and August) due to the academic break. Furthermore, the building remains largely closed during this period, which likely restricts the infiltration of outdoor air pollutants. These conditions collectively reduce the seasonal contrast indoors, despite the evident fluctuations in outdoor air quality. Figure 3 presents the time series of  $PM_{2.5}$  concentrations.

XRD and SEM/EDS results provided information about crystallographic phases and compounds that exist in the indoor atmosphere. Supporting Information 1: Figure S1 shows a representative XRD pattern for Sample #76. The figure shows major phases commonly observed in  $PM_{2.5}$  such as manganite ( $(\text{NH}_4)_2\text{SO}_4$ ), kokaite ( $(\text{NH}_4)_2\text{Ca}(\text{SO}_4)_2(\text{H}_2\text{O})$ ), sodium sulfate hydrate ( $\text{Na}_2\text{SO}_4 \cdot 10\text{H}_2\text{O}$ ), calcite ( $\text{CaCO}_3$ ), and quartz ( $\text{SiO}_2$ ).

Supporting Information 1: Figure S2 presents representative SEM/EDS maps, which clearly indicate the presence of sodium chloride (halite) and nitrates. In alignment with the XRD findings, the maps also confirm the presence of calcite and quartz. Additionally, natural crustal elements such as Mg, Al, and Fe are detected, representing the presence of other mineral phases such as chlorite and serpentine [46].

### 3.2 | Source Apportionment

The data required for input into the EPA PMF model include the concentration and uncertainty values of  $PM_{2.5}$  and its constituent elements. Uncertainty values for each species were obtained from EDXRF analysis, and a 20% value was applied to represent the random uncertainties associated with the elemental concentration data [47]. A total of 27 species were initially input into the model: PM, eBC, Na, Mg, Al, Si, P, S, Cl, K, Ca, Ti, V, Cr, Mn, Fe, Ni, Cu, Zn, Ga, As, Br, Rb, Sr, Zr, Ba, and Pb. All concentrations are expressed in  $\mu\text{g}/\text{m}^3$ .

Species with an S/N ratio below 0.5 (Cr, Ga, As, Rb, and Zr) were classified as “bad” and excluded from the model run. Additionally, species (eBC, Na, K, Cu, Zn, Br, Ba, and Pb) were marked as “weak” due to significant discrepancies between observed and modeled concentrations.  $PM_{2.5}$  mass was designated as the “total variable,” which by default is treated as weak in the model. All weak species had their uncertainty values multiplied by a factor of 3 to reduce their influence on the final solution [33].

The model was run 100 times with an additional modeling uncertainty of 5%. Factor numbers were varied from 3 to 9 in exploratory runs to identify the most physically interpretable and statistically robust solution. A six-factor solution was selected as optimal, yielding a correlation coefficient of 0.64 between observed and predicted PM mass concentrations. This moderate correlation is attributed to the assignment of the total measured PM mass as “weak” in the model input.

All species in the selected solution exhibited  $Q/Q_{\text{exp}}$  values less than 2, indicating acceptable model performance. DISP analysis showed minimal change in  $Q$  value and zero factor swapping at the lowest displacement level ( $dQ_{\text{max}} = 4$ ), which

**TABLE 1** | Mean, minimum, maximum, and standard deviation of PM<sub>2.5</sub> and its constituent elemental concentrations.

	Mean ( $\mu\text{g}/\text{m}^{-3}$ )	Min ( $\mu\text{g}/\text{m}^{-3}$ )	Max ( $\mu\text{g}/\text{m}^{-3}$ )	SD ( $\mu\text{g}/\text{m}^{-3}$ )
PM <sub>2.5</sub>	14.937	6.292	29.257	4.812
eBC	0.607	0.085	1.359	0.271
Na	0.102	0.040	0.220	0.040
Mg	0.067	0.020	0.296	0.044
Al	0.111	0.021	0.610	0.079
Si	0.292	0.040	1.731	0.228
P	0.198	0.030	0.501	0.101
S	1.753	0.313	6.390	1.184
Cl	0.027	0.005	0.116	0.018
K	0.098	0.025	0.291	0.038
Ca	0.246	0.050	1.131	0.166
Ti	0.008	0.001	0.041	0.006
V	0.003	0.000	0.010	0.002
Cr	0.001	0.000	0.003	0.001
Mn	0.004	0.000	0.014	0.002
Fe	0.136	0.043	0.561	0.070
Ni	0.002	0.000	0.008	0.001
Cu	0.002	0.000	0.010	0.002
Zn	0.026	0.003	0.073	0.015
Br	0.003	0.000	0.013	0.002
Sr	0.002	0.000	0.009	0.002
Ba	0.004	0.000	0.020	0.003
Pb	0.008	0.000	0.126	0.014

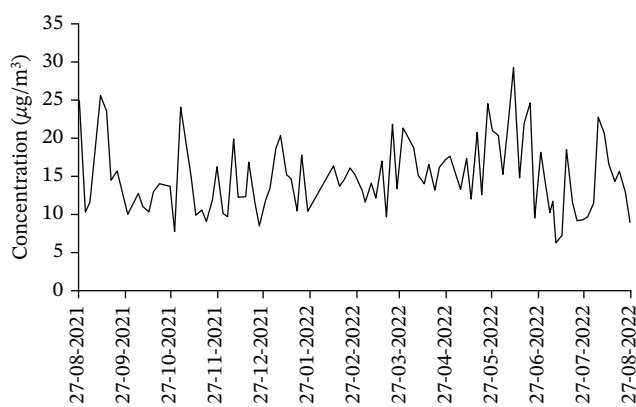


**FIGURE 3** | Time series of PM<sub>2.5</sub> concentrations.

suggests stability of the solution. BS analysis (400 runs,  $R \geq 0.8$ ) revealed that all bootstrap factors were consistently mapped to their corresponding base factor. The mapping accuracy

ranged from 84% to 100% for the factors, indicating good solution stability [33]. These diagnostics confirm the robustness of the selected six-factor PMF solution. PMF base runs, settings, and results from error estimation are summarized in Supporting Information 1: Table S4. Supporting Information 1: Figures S3 and S4 show the observed and model-predicted concentration analysis of total PM<sub>2.5</sub> and selected elements. The source profiles for PM<sub>2.5</sub> are illustrated in Figure 4, where the percentage contribution of each species to the respective source factor is represented by red boxes, and the species concentrations in  $\mu\text{g}/\text{m}^3$  are shown as vertical bars. The left y-axis (logarithmic scale) corresponds to the concentration bars, while the right y-axis represents the species percentage contribution [33]. The six source factors identified were heavy oil combustion (HOC), sea salt, RD, secondary aerosol (SA), traffic, and mineral dust. This shows that the intrusion of outdoor pollutants is the major contributor to IAQ depletion in the university building. Supporting Information 1: Figure S5 shows the factor contribution to total PM<sub>2.5</sub>.

RD comprises 11.7% of the PM mass and is marked by the presence of Mg, Al, Si, Ca, Fe, and Sr, alongside lower levels of Ti and Mn [48, 49]. Many of these are crustal elements commonly linked to soil and construction-related activities. In particular, Sr, Mg, and Ca are often associated with dust from construction sites [50]. In fact, the study site (University City in Sharjah) is in proximity to several large-scale construction projects located within 1–2 miles. Therefore, the source likely reflects both crustal resuspension and ongoing construction dust.

The most dominant source identified in this study is SA formation, contributing 33.4% of the total PM<sub>2.5</sub> mass. This factor includes high levels of S and P, along with considerable concentrations of eBC [48, 51, 52]. The observed eBC within this factor likely arises from cross-loading of combustion-related components into the SA profile. The sulfate-rich SA primarily originates from anthropogenic sources such as shipping activities and fuel combustion, hence the high levels of eBC observed within this source [53, 54]. These activities emit gaseous precursors, such as SO<sub>2</sub>, which undergo atmospheric oxidation to form sulfuric acid. Sulfuric acid reacts with ambient ammonia to produce ammonium sulfate ((NH<sub>4</sub>)<sub>2</sub>SO<sub>4</sub>). In the UAE, high solar radiation and elevated temperatures enhance photochemical activity, accelerating sulfate formation. The region's major SO<sub>2</sub> sources include power plants, vehicle emissions, and port-related marine traffic [24]. The consistent presence of sulfate-rich particles indoors indicates infiltration of these outdoor-derived secondary pollutants.

Sea salt is an identified contributor, constituting 9.2% of the PM<sub>2.5</sub> mass. This source is primarily distinguished by high levels of Na and Cl, with low levels of Mg [55, 56]. The Na/Cl ratio obtained from elemental concentrations is 3.8, indicating a higher abundance of sodium compared to typical marine aerosols. This is likely due to the presence of sodium nitrate, consistent with outdoor chemical transformation processes, which has been observed in an outdoor study in the vicinity of the building [24]. Given that the sampling site is located approximately 7 km from the coastline, sea salt is considered to be marine aerosol that has infiltrated indoors.

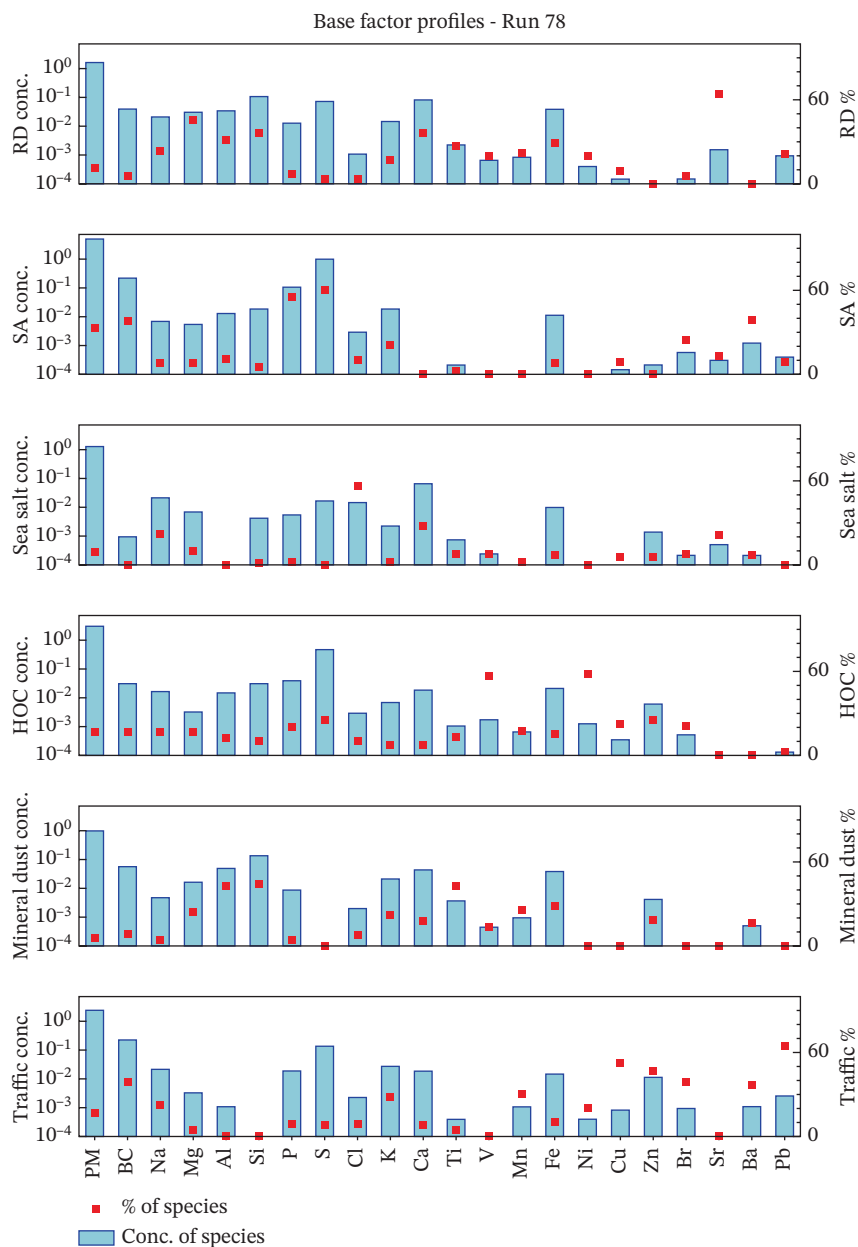


**FIGURE 4** | Source profiles of indoor  $PM_{2.5}$ .

One of the major sources contributing to indoor  $PM_{2.5}$  is HOC, accounting for 22.2% of the total  $PM_{2.5}$  mass. This source is characterized by elevated concentrations of V and Ni, which are well-established tracers for HOC emissions [57, 58]. Since there are no such indoor combustion sources in the academic building, this factor is attributed to outdoor infiltration from marine shipping activities along the Gulf Coast.

Mineral dust is another contributor that accounts for 6.6% of the PM mass and is rich in Al, Si, Fe, Ti, Ca, K, and Mg [48, 58]. These, along with moderate amounts of Mn, are widely recognized as crustal elements, typically originating from mineral soils, as the region is adjacent to deserts [50, 56]. Additionally, V appears in this profile and is consistent with findings from regional dust studies, suggesting a crustal or natural origin [24].

Traffic emissions contribute 16.8% of the PM mass, with this factor showing high concentrations of eBC, Cu, Zn, Br, Ba, and Pb, alongside smaller amounts of Mn and Fe. All of these elements are commonly linked to vehicular activity, including exhaust emissions with incomplete fossil fuel combustion and nonexhaust emissions such as brake and tire wear [48, 49, 55].

All the identified sources determined from elemental analysis point to the intrusion of outdoor atmospheric pollutants, consistent with the building’s location and ventilation setup. Infiltration pathways likely include air-conditioning systems, doors, windows, cracks, and resuspension through foot traffic. This assessment explains the effect of outdoor pollutants on the IAQ. The PMF results indicate that 72% of indoor contaminants are anthropogenic in origin, while 28% are natural. This emphasizes the importance of monitoring and mitigating ambient air

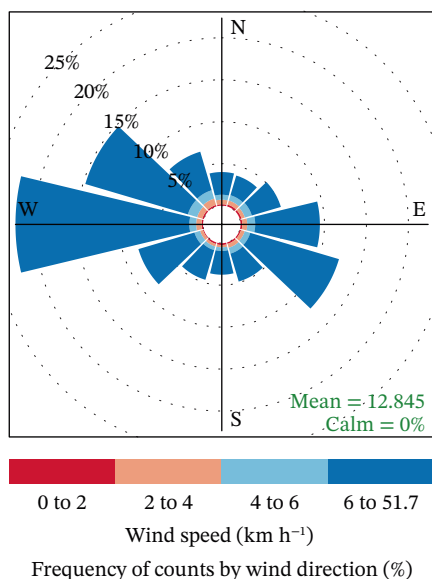


**FIGURE 5** | Wind rose showing wind speed, direction, and frequency for the Physics Department at the American University of Sharjah during the study period, based on hourly wind data.

pollutants, as well as implementing effective structural management and filtration systems within indoor environments.

Figure 5 presents the wind rose for the sampling period, showing that westerly and northwesterly winds dominate at the site, with additional contributions from southeasterly and easterly directions. Given the location of the site between the Arabian Gulf and an extensive desert area, it is reasonable to expect source contributions similar to those identified in a nearby outdoor study within 4 km [47]. These wind patterns are consistent with the PMF source apportionment results, suggesting contributions from marine activities (e.g., HOC and sea salt) associated with northwesterly winds, as well as mineral dust transported from desert regions to the east and southeast. SAs are likely influenced by long-range transport from the northwestern region, where industrial and marine activities, along with onshore and offshore oil extraction and refining, emit precursor gases such as  $\text{SO}_2$  and  $\text{NO}_x$  [47]. In addition, local sources, including traffic emissions and construction-related dust, are expected given the urban setting and ongoing infrastructure development.

### 3.3 | Health Risk Assessment

#### 3.3.1 | Noncarcinogenic Risk

The EF was calculated to be 0.18. The calculated EF-AACs and the HQ values are shown in Table 2. All nine elements analyzed (Cr, Mn, Al, As, Cu, Ni, Pb, Zn, and Mg) were found to have an HQ value less than 1, which, according to the Agency for Toxic Substances and Disease Registry (ATSDR) guidelines [39], indicates that there is no significant noncarcinogenic health risk. The elements arranged in decreasing order of HQ are  $\text{Mn} > \text{Zn} > \text{Al} > \text{Cu} > \text{Cr} > \text{Pb} > \text{As} > \text{Ni} > \text{Mg}$ . Among these elements, Al and Zn have comparatively higher mean concentrations, indicating that their major sources, mineral dust and traffic, contribute to the indoor environment.

#### 3.3.2 | Carcinogenic Risk

The calculated carcinogenic risk of carcinogenic elements (As, Cr, Ni, and Pb) is given in Table 3. All elements show a carcinogenic risk below  $1 \times 10^{-6}$  for both male and female occupants, which is the threshold value recommended by the ATSDR. For all the carcinogens, females showed a lower risk of exposure than males. Among the analyzed elements, Cr showed the highest CR values,  $9.5 \times 10^{-8}$  for males and  $9.1 \times 10^{-8}$  for females, which are still nearly 10 times lower than the threshold value. The Cr content was assumed to be Cr(VI) in the atmosphere since our current analysis does not differentiate between oxidation states, and this assumption helps to assess the highest exposure risk.

The health risk assessment results of this study are consistent with other indoor PM studies, suggesting that health risks associated with PM are generally limited in the absence of strong indoor emission sources. Both noncarcinogenic and carcinogenic risks were found to be within acceptable limits for the study conducted in university dormitories in Nanjing, China [59]. Concentrations of indoor air pollutants from 88 studies in a residential setting in the United States were compared in [60], and trace metals were found to be within acceptable limits. In contrast, elevated health risks have been reported in indoor environments with combustion. A yearlong study in rural Northeast China demonstrated indoor metal concentrations that are substantially higher, resulting in carcinogenic and noncarcinogenic risks. The CR values were above  $10^{-4}$ , and a higher risk was found for children [61]. However, specialized occupational microenvironments, such as academic metallurgy workshops, reported elevated HQ values ( $> 1$ ) and CR values ( $> 10^{-6}$ ) for certain occupants [42]. The comparatively low HQ and CR values observed in the current study indicate that the studied environment poses no serious threat in the context of the global IAQ spectrum.

### 3.4 | Analysis Using MPPD

The deposition, clearance, and retention of PM in the human respiratory tract were analyzed using the MPPD model for individuals aged 18 and 21 years old in the university indoor environment scenario. Figures 6a and 7a illustrate the lung geometry visualizations for both age groups. Figures 6b and 7b depict the visual representation of PM deposition in the alveolar region. As shown, both age groups experience high particle deposition in the lower pulmonary area.  $\text{PM}_{2.5}$  is more likely to deposit in this region compared to coarse particles ( $\text{PM}_{10}$ ) and can potentially penetrate the alveolar barrier, allowing translocation to other organs [62]. Figures 6c and 7c show the deposition fraction of  $\text{PM}_{2.5}$  within the respiratory system. Deposition fraction refers to the proportion of inhaled aerosol mass deposited in specific regions of the respiratory tract [63]. The analysis reveals that approximately 75% of inhaled  $\text{PM}_{2.5}$  is deposited at various sites within the respiratory system for both age groups, with slightly lower deposition observed in 18-year-olds.

More than 40% of the total inhaled PM is deposited in the head region, with 18-year-olds exhibiting a slightly higher deposition in this area than 21-year-olds. A similar trend is observed in the tracheobronchial (TB) region, where deposition is over 5% for 18-year-olds, compared to 4.7% for 21-year-olds. This greater

**TABLE 2** | EF-adjusted air concentrations and the hazard quotient values for noncarcinogenic elements.

	Cr	Mn	Al	As	Cu	Ni	Pb	Zn	Mg
AAC	$1.02 \times 10^{-4}$	$6.74 \times 10^{-4}$	$2.03 \times 10^{-2}$	$9.57 \times 10^{-5}$	$4.12 \times 10^{-4}$	$3.72 \times 10^{-4}$	$1.51 \times 10^{-3}$	$4.83 \times 10^{-3}$	$1.22 \times 10^{-2}$
HQ	$3.42 \times 10^{-3}$	$1.35 \times 10^{-2}$	$4.07 \times 10^{-3}$	$3.19 \times 10^{-4}$	$3.43 \times 10^{-3}$	$2.66 \times 10^{-5}$	$2.90 \times 10^{-3}$	$1.34 \times 10^{-2}$	$2.99 \times 10^{-6}$

**TABLE 3** | EF-adjusted air concentrations and the carcinogenic risk values for carcinogenic elements.

		As	Cr	Ni	Pb
AAC		$9.57 \times 10^{-5}$	$1.02 \times 10^{-4}$	$3.72 \times 10^{-4}$	$1.51 \times 10^{-3}$
CR	Male	$2.13 \times 10^{-8}$	$9.58 \times 10^{-8}$	$4.63 \times 10^{-9}$	$9.39 \times 10^{-10}$
	Female	$2.06 \times 10^{-8}$	$9.24 \times 10^{-8}$	$4.47 \times 10^{-9}$	$9.06 \times 10^{-10}$

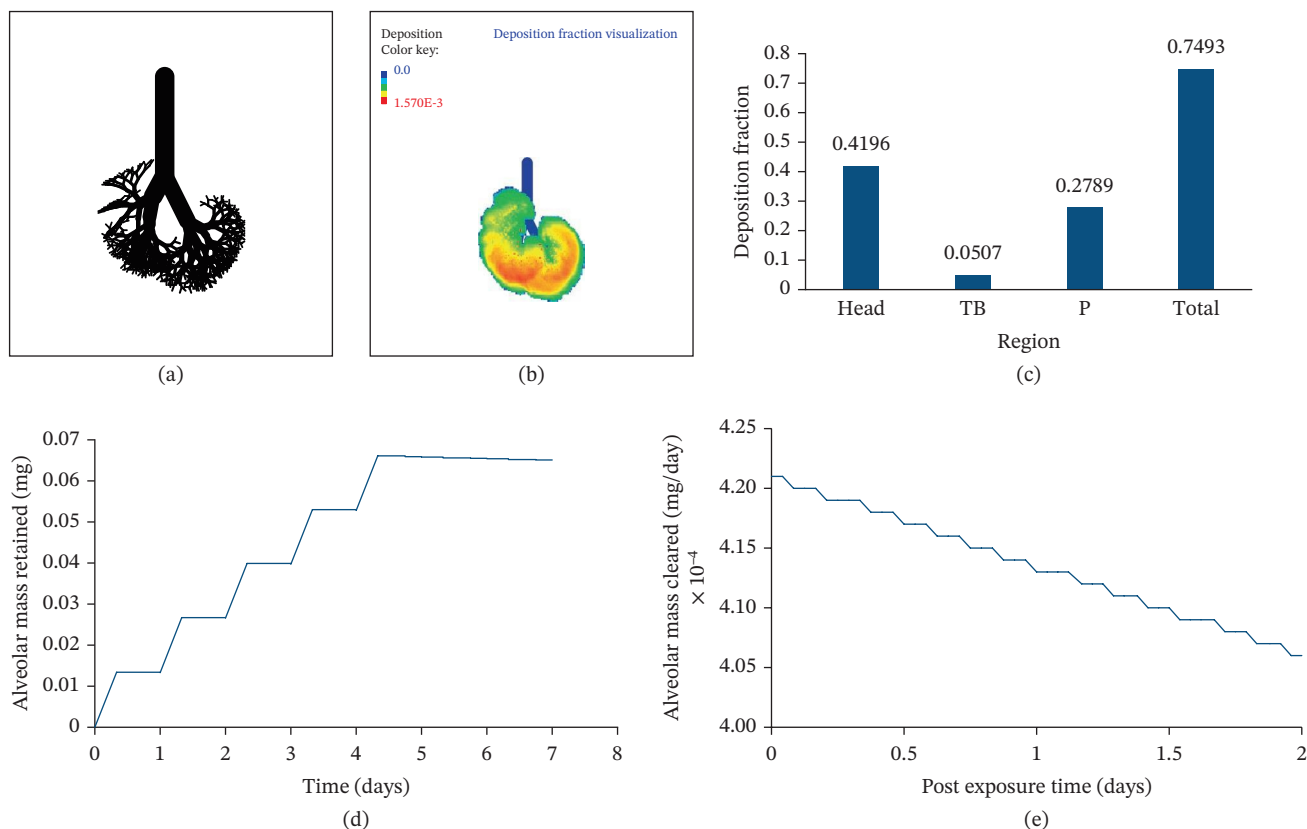


**FIGURE 6** | (a) Lung geometry visualization (for adults aged 18 years old), (b) visual representation of PM<sub>2.5</sub> depositions in the alveolar region, (c) deposition fraction of PM<sub>2.5</sub> within the respiratory system, (d) alveolar mass retention, and (e) alveolar mass clearance.

deposition in the upper airways among younger individuals results in a reduced fraction reaching the pulmonary region, about 2% lower than that in 21-year-olds. These observations are consistent with previous studies that have reported higher PM deposition in the head region [64–66].

Figures 6d,e and 7d,e present the alveolar mass clearance and retention, respectively. Alveolar clearance represents the total PM mass removed daily from the alveoli via biological processes. The model estimates a daily clearance of 0.00045 mg for 21-year-olds and 0.00041 mg for 18-year-olds. These results

assume no additional particle deposition during the clearance period. The mass retention curve increases during the exposure period due to continuous PM deposition. After 5 days of exposure, the alveolar region retains 0.072 mg of PM in 21-year-olds and 0.066 mg in 18-year-olds.

Overall, the analysis characterizes PM deposition under an indoor university building scenario and suggests a comparatively higher alveolar burden in the older age group within this modeled exposure context. Prolonged retention of PM in the alveolar region is concerning, as sustained interaction of particles

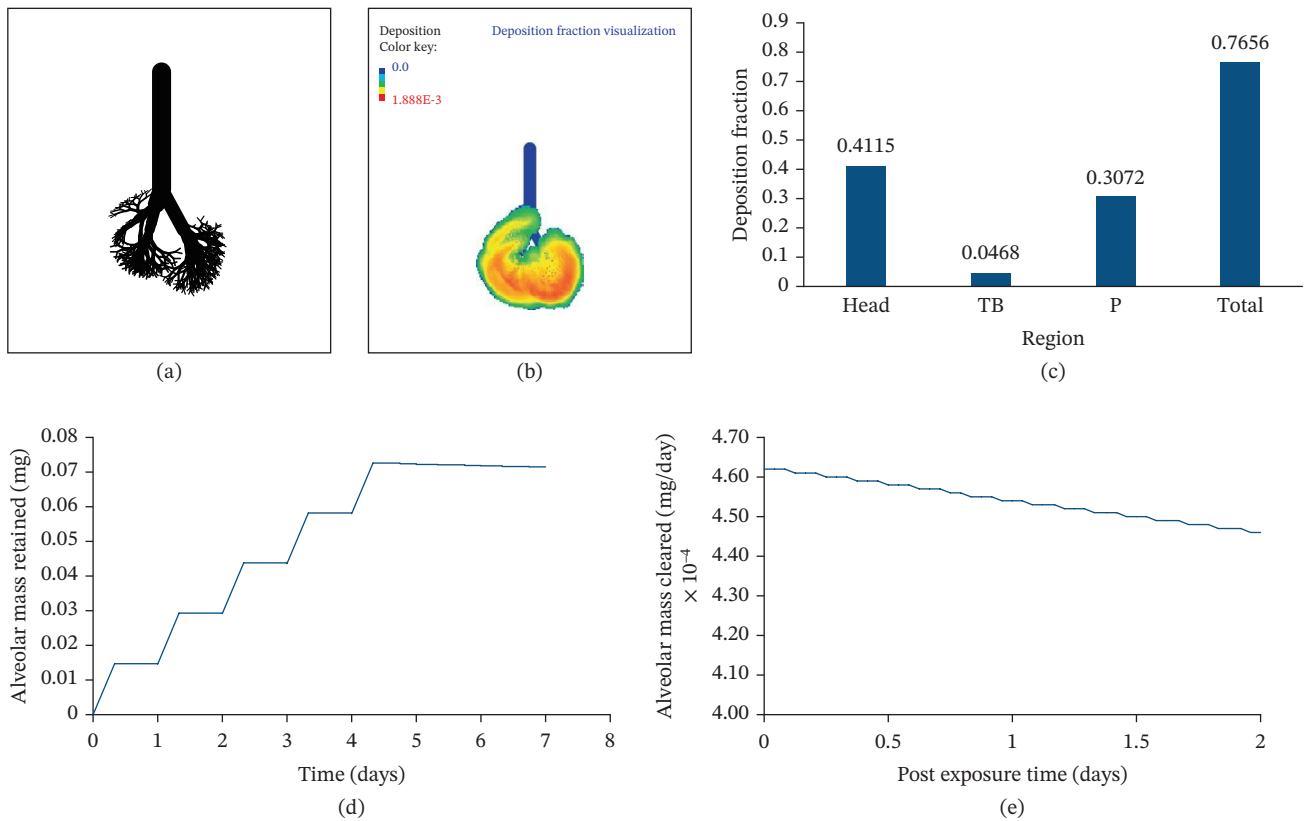


**FIGURE 7** | (a) Lung geometry visualization (for adults aged 21 years old), (b) visual representation of  $PM_{2.5}$  depositions in the alveolar region, (c) deposition fraction of  $PM_{2.5}$  within the respiratory system, (d) alveolar mass retention, and (e) alveolar mass clearance.

with the alveolar epithelial cells and macrophages leads to chronic inflammation and oxidative stress [67]. Previous epidemiological evidence indicates that inefficient alveolar clearance and long-term retention are associated with increased susceptibility to obstructive lung diseases and elevated risks of cardiopulmonary morbidity, which becomes particularly relevant under the chronic exposure scenario of the university building [68].

#### 4 | Conclusion

This study provides the first indoor  $PM_{2.5}$  pollutant study in the Middle East that integrates detailed elemental characterization, chemical speciation, and source apportionment using advanced analytical methods and health impact assessments. The results show that indoor air in the academic building under study is significantly influenced by outdoor sources such as mineral and RD (18.9%), sea salt (8.6%), and anthropogenic sources, like SAs (34.2%), traffic (17.2%), and HOC (21.1%). Wind rose analysis further confirms that the dominant westerly/northwesterly and easterly airflows are consistent with the identified marine, heavy oil, and dust-related source contributions. This emphasizes that the indoor pollutants of the current study are mainly influenced by outdoor sources. Out of nine measured heavy metal elements (Cr, Mn, Al, As, Cu, Ni, Pb, Zn, and Mg), none exceeded the recommended noncarcinogenic risk threshold value. Also, four measured trace elements (As, Cr, Ni, and Pb) showed carcinogenic risk values less than the threshold value. MPPD modeling showed the age-specific

deposition of PM in the respiratory tract: 21-year-olds showed slightly higher deposition (nearly 75%) than 18-year-olds, with 41.1% deposition in the head region, 4.7% in the TB region, and 30.7% in the pulmonary region. They also have a higher retention of the particulate pollutants, indicating an increased risk with age. This can be linked with the lower rate of alveolar clearance for the 21-year-olds. In future studies, to overcome some limitations associated with the current study, we suggest including organic nonmetallic components and water-soluble ions in the analysis to achieve more optimal source identification. Also, incorporating multiple sites will provide a more comprehensive understanding of the effect of  $PM_{2.5}$  on health. These findings emphasize the need for regular and continuous monitoring and source control strategies for both indoor and outdoor ambient air. Targeted interventions such as improved filtration, ventilation, and IAQ regulations can also play a crucial role in safeguarding occupant health and ensuring a healthier environment in indoor settings.

#### Author Contributions

**Shahid Anwar:** writing – review and editing, writing – original draft, visualization, validation, software, methodology, investigation, formal analysis, data curation. **Vipin Satheesh:** writing – review and editing, writing – original draft, visualization, validation, software, methodology, investigation, formal analysis, data curation. **Nasser M. Hamdan:** writing – review and editing, visualization, validation, supervision, resources, project administration, formal analysis, conceptualization. **Mohamed Shameer:** elemental analysis, writing – review and editing. **Hussain Alawadhi:** writing – review and editing.

## Acknowledgments

N.M.H. would like to acknowledge the AUS Office of Research for support through project number 223209. He also acknowledges the support received from the Division for Asia and the Pacific, Department of Technical Cooperation, International Atomic Energy Agency (IAEA), Vienna. The authors thank Mr. Muhammed Irshad Shahul Hameed at the Research Institute of Sciences and Engineering, University of Sharjah, for performing XRD experiments. The authors declare that they have not used any generative AI-assisted technology in writing this article. This paper represents the opinions of the authors and does not mean to represent the position or opinions of the American University of Sharjah.

## Funding

The AUS Office of Research provided support through project number 223209.

## Disclosure

The authors take full responsibility for the content of this paper.

## Conflicts of Interest

The authors declare no conflicts of interest.

## Data Availability Statement

The data that support the findings of this study are available from the corresponding author upon reasonable request.

## References

1. D. Saraga, S. Pateraki, A. Papadopoulos, C. Vasilakos, and T. Maggos, "Studying the Indoor Air Quality in Three Non-Residential Environments of Different Use: A Museum, a Printery Industry and an Office," *Building and Environment* 46, no. 11 (2011): 2333–2341, <https://doi.org/10.1016/j.buildenv.2011.05.013>.
2. A. H. Goldstein, W. W. Nazaroff, C. J. Weschler, and J. Williams, "How Do Indoor Environments Affect Air Pollution Exposure?," *Environmental Science & Technology* 55, no. 1 (2021): 100–108, <https://doi.org/10.1021/acs.est.0c05727>.
3. M. Wang, C. P. Aaron, J. Madrigano, et al., "Association Between Long-Term Exposure to Ambient Air Pollution and Change in Quantitatively Assessed Emphysema and Lung Function," *Journal of the American Medical Association* 322, no. 6 (2019): 546–556, <https://doi.org/10.1001/jama.2019.10255>.
4. S. E. Alexeeff, K. Deosaransingh, S. Van Den Eeden, J. Schwartz, N. S. Liao, and S. Sidney, "Association of Long-Term Exposure to Particulate Air Pollution With Cardiovascular Events in California," *JAMA Network Open* 6, no. 2 (2023): e230561, <https://doi.org/10.1001/jamanetworkopen.2023.0561>.
5. WHO, "Health Data Overview for the United Arab Emirates," (2026), <https://data.who.int/countries/784>.
6. H. Razzak, A. Harbi, S. Ahli, and W. Shelpai, "Chronic Obstructive Pulmonary Disease; Prevalence and Associated Risk Factors in the United Arab Emirates," *Hamdan Medical Journal* 13, no. 1 (2020): 20, [https://doi.org/10.4103/HMJ.HMJ\\_27\\_19](https://doi.org/10.4103/HMJ.HMJ_27_19).
7. P. Yu, R. Xu, M. S. Z. S. Coelho, et al., "The Impacts of Long-Term Exposure to PM<sub>2.5</sub> on Cancer Hospitalizations in Brazil," *Environment International* 154 (2021): 106671, <https://doi.org/10.1016/j.envint.2021.106671>.
8. C. M. Wong, H. Tsang, H. K. Lai, et al., "Cancer Mortality Risks From Long-Term Exposure to Ambient Fine Particle," *Cancer Epidemiology, Biomarkers & Prevention* 25, no. 5 (2016): 839–845, <https://doi.org/10.1158/1055-9965.EPI-15-0626>.

9. O. Toyinbo, L. Hägerhed, S. Dimitroulopoulou, et al., "Open Database for International and National Indoor Environmental Quality Guidelines," *Indoor Air* 32, no. 4 (2022): e13028, <https://doi.org/10.1111/ina.13028e13028>.
10. R. Zhang, X. He, J. Liu, and J. Xiong, "VOC Transport in an Occupied Residence: Measurements and Predictions via Deep Learning," *Science of the Total Environment* 892 (2023): 164559, <https://doi.org/10.1016/j.scitotenv.2023.164559>.
11. R. Camilleri, A. J. Vella, R. M. Harrison, and N. J. Aquilina, "Source Apportionment of Indoor PM<sub>2.5</sub> at a Residential Urban Background Site in Malta," *Atmospheric Environment* 278 (2022): 119093, <https://doi.org/10.1016/j.atmosenv.2022.119093>.
12. I. Nezis, G. Biskos, K. Eleftheriadis, and O.-I. Kalantzi, "Particulate Matter and Health Effects in Offices - A Review," *Building and Environment* 156 (2019): 62–73, <https://doi.org/10.1016/j.buildenv.2019.03.042>.
13. B. M. Roberts, D. Allinson, and K. J. Lomas, "Evaluating Methods for Estimating Whole House Air Infiltration Rates in Summer: Implications for Overheating and Indoor Air Quality," *International Journal of Building Pathology and Adaptation* 41, no. 1 (2023): 45–72, <https://doi.org/10.1108/IJBPA-06-2021-0085>.
14. Y. Yang, L. Liu, C. Xu, et al., "Source Apportionment and Influencing Factor Analysis of Residential Indoor PM<sub>2.5</sub> in Beijing," *International Journal of Environmental Research and Public Health* 15, no. 4 (2018): 686, <https://doi.org/10.3390/ijerph15040686>.
15. J. N. M. Zhong, M. T. Latif, N. Mohamad, N. B. A. Wahid, D. Dominick, and H. Juahir, "Source Apportionment of Particulate Matter (PM<sub>10</sub>) and Indoor Dust in a University Building," *Environmental Forensics* 15, no. 1 (2014): 8–16, <https://doi.org/10.1080/15275922.2013.872712>.
16. C. Li, L. Bai, Z. He, and Y. Wang, "Health Risk Assessment of Heavy Metals and Poly-Aromatic Hydrocarbons in Particulate Matter Adsorbed by Indoor Air Purifiers," *Indoor and Built Environment* 31, no. 6 (2022): 1594–1612, <https://doi.org/10.1177/1420326X211052239>.
17. L. O. Gostin, J. G. Hodge, and G. K. Gronvall, "The Model State Indoor Air Quality Act," *Journal of the American Medical Association* 330, no. 16 (2023): 1525–1526, <https://doi.org/10.1001/jama.2023.17334>.
18. WHO, "WHO Guidelines for Indoor Air Quality: Selected Pollutants," (2010), <https://www.who.int/publications/i/item/9789289002134>.
19. D. E. Saraga, X. Querol, R. M. B. O. Duarte, et al., "Source Apportionment for Indoor Air Pollution: Current Challenges and Future Directions," *Science of the Total Environment* 900 (2023): 165744, <https://doi.org/10.1016/j.scitotenv.2023.165744>.
20. C. Li, L. Bai, H. Wang, and Z. Li, "Promoting the Design of Future Urban Metro Systems to Improve Air Pollution: Based on Metal Element Pollution in Chinese Metro System," *Sustainable Cities and Society* 97 (2023): 104753, <https://doi.org/10.1016/j.scs.2023.104753>.
21. M. Y. Ali, M. M. Hanafiah, M. F. Khan, and M. T. Latif, "Quantitative Source Apportionment and Human Toxicity of Indoor Trace Metals at University Buildings," *Building and Environment* 121 (2017): 238–246, <https://doi.org/10.1016/j.buildenv.2017.05.032>.
22. N. Hamdan, H. Alawadhi, N. Jisrawi, and M. Shameer, "Characterization of Fine Particulate Matter in Sharjah, United Arab Emirates Using Complementary Experimental Techniques," *Sustainability* 10, no. 4 (2018): 1088, <https://doi.org/10.3390/su10041088>.
23. N. M. Hamdan, H. Alawadhi, N. Jisrawi, and M. Shameer, "Size-Resolved Analysis of Fine and Ultrafine Fractions of Indoor Particulate Matter Using Energy Dispersive X-ray Fluorescence and Electron Microscopy," *X-Ray Spectrometry* 47, no. 1 (2018): 72–78, <https://doi.org/10.1002/xrs.2813>.
24. N. M. Hamdan, H. Alawadhi, and M. Shameer, "Characterization of PM<sub>2.5</sub> at a Traffic Site Using Several Integrated Analytical Techniques,"

- X-Ray Spectrometry 50, no. 2 (2021): 106–120, <https://doi.org/10.1002/xrs.3201>.
25. N. M. Hamdan, H. Alawadhi, and M. Shameer, “Physicochemical Characterization and Seasonal Variations of PM<sub>10</sub> Aerosols in a Harsh Environment,” *Frontiers in Environmental Science* 9 (2021): 666678, <https://doi.org/10.3389/fenvs.2021.666678>.
26. W. E. May, and J. Rumble, *Certificate of Analysis–Standard Reference Material 2780 - Hard Rock Mine Waste* (National Institute of Standards and Technology, 2003).
27. N. M. Hamdan, H. Alawadhi, and N. Jisrawi, “Particulate Matter Pollution in the United Arab Emirates: Elemental Analysis and Phase Identification of Fine Particulate Pollutants,” (2016), <https://doi.org/10.11159/icepr16.158>.
28. P. M. Davy, A. H. Tremper, E. M. G. Nicolosi, P. Quincey, and G. W. Fuller, “Estimating Particulate Black Carbon Concentrations Using Two Offline Light Absorption Methods Applied to Four Types of Filter Media,” *Atmospheric Environment* 152 (2017): 24–33, <https://doi.org/10.1016/j.atmosenv.2016.12.010>.
29. P. Paatero, and P. K. Hopke, “Discarding or Downweighting High-Noise Variables in Factor Analytic Models,” *Analytica Chimica Acta* 490, no. 1–2 (2003): 277–289, [https://doi.org/10.1016/S0003-2670\(02\)01643-4](https://doi.org/10.1016/S0003-2670(02)01643-4).
30. P. Paatero, and U. Tapper, “Positive Matrix Factorization: A Non-Negative Factor Model With Optimal Utilization of Error Estimates of Data Values,” *Environmetrics* 5, no. 2 (1994): 111–126, <https://doi.org/10.1002/env.3170050203>.
31. M. Manousakas, E. Diapouli, H. Papaefthymiou, et al., “Source Apportionment by PMF on Elemental Concentrations Obtained by PIXE Analysis of PM<sub>10</sub> Samples Collected at the Vicinity of Lignite Power Plants and Mines in Megalopolis, Greece,” *Nuclear Instruments and Methods in Physics Research Section B* 349 (2015): 114–124, <https://doi.org/10.1016/j.nimb.2015.02.037>.
32. M. Manousakas, H. Papaefthymiou, E. Diapouli, et al., “Assessment of PM<sub>2.5</sub> Sources and Their Corresponding Level of Uncertainty in a Coastal Urban Area Using EPA PMF 5.0 Enhanced Diagnostics,” *Science of the Total Environment* 574 (2017): 155–164, <https://doi.org/10.1016/j.scitotenv.2016.09.047>.
33. G. Norris, R. Duvall, S. Brown, and S. Bai, “EPA Positive Matrix Factorization (PM F) 5.0 Fundamentals and User Guide,” (2014), [https://www.epa.gov/sites/default/files/2015-02/documents/pmf\\_5.0\\_user\\_guide.pdf](https://www.epa.gov/sites/default/files/2015-02/documents/pmf_5.0_user_guide.pdf).
34. S. Esmaeilirad, A. Lai, G. Abbaszade, et al., “Source Apportionment of Fine Particulate Matter in a Middle Eastern Metropolis, Tehran-Iran, Using PMF With Organic and Inorganic Markers,” *Science of the Total Environment* 705 (2020): 135330, <https://doi.org/10.1016/j.scitotenv.2019.135330>.
35. G. Grivas, S. Cheristanidis, A. Chaloulakou, P. Koutrakis, and N. Mihalopoulos, “Elemental Composition and Source Apportionment of Fine and Coarse Particles at Traffic and Urban Background Locations in Athens, Greece,” *Aerosol and Air Quality Research* 18, no. 7 (2018): 1642–1659, <https://doi.org/10.4209/aaqr.2017.12.0567>.
36. S. G. Brown, S. Eberly, P. Paatero, and G. A. Norris, “Methods for Estimating Uncertainty in PMF Solutions: Examples With Ambient Air and Water Quality Data and Guidance on Reporting PMF Results,” *Science of the Total Environment* 518–519 (2015): 626–635, <https://doi.org/10.1016/j.scitotenv.2015.01.022>.
37. “NASA Langley Research Center. The Power Project,” (2026), <https://power.larc.nasa.gov/>.
38. L. Wu, X. S. Luo, H. Li, et al., “Seasonal Levels, Sources, and Health Risks of Heavy Metals in Atmospheric PM<sub>2.5</sub> From Four Functional Areas of Nanjing City, Eastern China,” *Atmosphere* 10, no. 7 (2019): 419, <https://doi.org/10.3390/atmos10070419>.
39. ““Calculating Hazard Quotients and Cancer Risk Estimates,” Agency for Toxic Substances and Disease Registry,” (2025), [https://atsdr.cdc.gov/pha-guidance/conducting\\_scientific\\_evaluations/epcs\\_and\\_exposure\\_calculations/hazardquotients\\_cancerrisk.html](https://atsdr.cdc.gov/pha-guidance/conducting_scientific_evaluations/epcs_and_exposure_calculations/hazardquotients_cancerrisk.html).
40. California Office of Environmental Health Hazard Assessment, “Lead and Lead Compounds: Inhalation Unit Risk and Potency Factors,” (2025), <https://oehha.ca.gov/chemicals/lead-and-lead-compounds>.
41. United Arab Emirates, “Health Data Overview for the United Arab Emirates World Health Organization 2025,” (2025), <https://data.who.int/countries/784>.
42. S. J. Mbazima, “Health Risk Assessment of Particulate Matter 2.5 in an Academic Metallurgy Workshop,” *Indoor Air* 32, no. 9 (2022): e13111, <https://doi.org/10.1111/ina.13111>.
43. C. Protano, M. Manigrasso, P. Avino, and M. Vitali, “Second-Hand Smoke Generated by Combustion and Electronic Smoking Devices Used in Real Scenarios: Ultrafine Particle Pollution and Age-Related Dose Assessment,” *Environment International* 107 (2017): 190–195, <https://doi.org/10.1016/j.envint.2017.07.014>.
44. F. J. Miller, B. Asgharian, J. D. Schroeter, and O. Price, “Improvements and Additions to the Multiple Path Particle Dosimetry Model,” *Journal of Aerosol Science* 99 (2016): 14–26, <https://doi.org/10.1016/j.jaerosci.2016.01.018>.
45. M. Manigrasso, M. Vitali, C. Protano, and P. Avino, “Ultrafine Particles in Domestic Environments: Regional Doses Deposited in the Human Respiratory System,” *Environment International* 118 (2018): 134–145, <https://doi.org/10.1016/j.envint.2018.05.049>.
46. N. M. Hamdan, and H. Alawadhi, “X-ray Diffraction as a Major Tool for the Analysis of PM<sub>2.5</sub> and PM<sub>10</sub> aerosols,” *Powder Diffraction* 35, no. 2 (2020): 98–103, <https://doi.org/10.1017/S0885715620000184>.
47. S. Anwar, M. Shameer, H. Alawadhi, and N. M. Hamdan, “Source Apportionment of PM<sub>2.5</sub> and PM<sub>10</sub> Pollutants Near an Urban Roadside Site Using Positive Matrix Factorization,” *Environmental Advances* 17 (2024): 100573, <https://doi.org/10.1016/j.envadv.2024.100573>.
48. W. Javed, and B. Guo, “Chemical Characterization and Source Apportionment of Fine and Coarse Atmospheric Particulate Matter in Doha, Qatar,” *Atmospheric Pollution Research* 12, no. 2 (2021): 122–136, <https://doi.org/10.1016/j.apr.2020.10.015>.
49. L. R. Crilley, F. Lucarelli, W. J. Bloss, et al., “Source Apportionment of Fine and Coarse Particles at a Roadside and Urban Background Site in London During the 2012 Summer ClearLo Campaign,” *Environmental Pollution* 220, pt. B (2017): 766–778, <https://doi.org/10.1016/j.envpol.2016.06.002>.
50. D. Srivastava, J. Xu, T. V. Vu, et al., “Insight Into PM<sub>2.5</sub> Sources by Applying Positive Matrix Factorization (PMF) at Urban and Rural Sites of Beijing,” *Atmospheric Chemistry and Physics* 21, no. 19 (2021): 14703–14724, <https://doi.org/10.5194/acp-21-14703-2021>.
51. D. Srivastava, S. Tomaz, O. Favez, et al., “Speciation of Organic Fraction Does Matter for Source Apportionment. Part 1: A One-Year Campaign in Grenoble (France),” *Science of the Total Environment* 624 (2018): 1598–1611, <https://doi.org/10.1016/j.scitotenv.2017.12.135>.
52. H. G. Ryou, J. Heo, and S.-Y. Kim, “Source Apportionment of PM<sub>10</sub> and PM<sub>2.5</sub> Air Pollution, and Possible Impacts of Study Characteristics in South Korea,” *Environmental Pollution* 240 (2018): 963–972, <https://doi.org/10.1016/j.envpol.2018.03.066>.
53. N. Jiang, S. Yin, Y. Guo, et al., “Characteristics of Mass Concentration, Chemical Composition, Source Apportionment of PM<sub>2.5</sub> and PM<sub>10</sub> and Health Risk Assessment in the Emerging Megacity in China,” *Atmospheric Pollution Research* 9, no. 2 (2018): 309–321, <https://doi.org/10.1016/j.apr.2017.07.005>.
54. I. Stanimirova, D. Q. Rich, A. G. Russell, and P. K. Hopke, “A Long-Term, Dispersion Normalized PMF Source Apportionment of PM<sub>2.5</sub>

in Atlanta From 2005 to 2019,” *Atmospheric Environment* 312 (2023): 120027, <https://doi.org/10.1016/j.atmosenv.2023.120027>.

55. S. Karnae, and K. John, “Source Apportionment of PM<sub>2.5</sub> Measured in South Texas Near U.S.A. – Mexico Border,” *Atmospheric Pollution Research* 10, no. 5 (2019): 1663–1676, <https://doi.org/10.1016/j.apr.2019.06.007>.

56. M. Alwadei, D. Srivastava, M. S. Alam, Z. Shi, and W. J. Bloss, “Chemical Characteristics and Source Apportionment of Particulate Matter (PM<sub>2.5</sub>) in Dammam, Saudi Arabia: Impact of Dust Storms,” *Atmospheric Environment: X* 14 (2022): 100164, <https://doi.org/10.1016/j.aeaoa.2022.100164>.

57. M. Masiol, P. K. Hopke, H. D. Felton, et al., “Source Apportionment of PM<sub>2.5</sub> Chemically Speciated Mass and Particle Number Concentrations in New York City,” *Atmospheric Environment* 148 (2017): 215–229, <https://doi.org/10.1016/j.atmosenv.2016.10.044>.

58. S. Jain, S. K. Sharma, N. Vijayan, and T. K. Mandal, “Seasonal Characteristics of Aerosols (PM<sub>2.5</sub> and PM<sub>10</sub>) and Their Source Apportionment Using PMF: A Four Year Study Over Delhi, India,” *Environmental Pollution* 262 (2020): 114337, <https://doi.org/10.1016/j.envpol.2020.114337>.

59. F. Wang, J. Wang, M. Han, C. Jia, and Y. Zhou, “Heavy Metal Characteristics and Health Risk Assessment of PM<sub>2.5</sub> in Students’ Dormitories in a University in Nanjing, China,” *Building and Environment* 160 (2019): 106206, <https://doi.org/10.1016/j.buildenv.2019.106206>.

60. J. M. Logue, T. E. McKone, M. H. Sherman, and B. C. Singer, “Hazard Assessment of Chemical Air Contaminants Measured in Residences,” *Indoor Air* 21, no. 2 (2011): 92–109, <https://doi.org/10.1111/j.1600-0668.2010.00683.x>.

61. C. Li, L. Bai, J. Qin, Y. Guo, H. Wang, and X. Xu, “Study on Metal Elements in Indoor Particulate Matter: A Case Study of Rural Residential Environment in Northeast China,” *Environmental Geochemistry and Health* 45, no. 7 (2023): 4867–4881, <https://doi.org/10.1007/s10653-023-01543-6>.

62. R. D. Arias-Pérez, N. A. Taborda, D. M. Gómez, J. F. Narvaez, J. Porras, and J. C. Hernandez, “Inflammatory Effects of Particulate Matter Air Pollution,” *Environmental Science and Pollution Research* 27, no. 34 (2020): 42390–42404, <https://doi.org/10.1007/s11356-020-10574-w>.

63. K.-H. Cheng, and D. L. Swift, “Calculation of Total Deposition Fraction of Ultrafine Aerosols in Human Extrathoracic and Intrathoracic Regions,” *Aerosol Science and Technology* 22, no. 2 (1995): 194–201, <https://doi.org/10.1080/02786829509508887>.

64. N. Manojkumar, B. Srimuruganandam, and S. M. Shiva Nagendra, “Application of Multiple-Path Particle Dosimetry Model for Quantifying Age Specified Deposition of Particulate Matter in Human Airway,” *Ecotoxicology and Environmental* 168 (2019): 241–248, <https://doi.org/10.1016/j.ecoenv.2018.10.091>.

65. N. Manojkumar, and B. Srimuruganandam, “Age-Specific and Seasonal Deposition of Outdoor and Indoor Particulate Matter in Human Respiratory Tract,” *Atmospheric Pollution Research* 13, no. 2 (2022): 101298, <https://doi.org/10.1016/j.apr.2021.101298>.

66. V. Martins, M. Cruz Minguillón, T. Moreno, et al., “Deposition of Aerosol Particles From a Subway Microenvironment in the Human Respiratory Tract,” *Journal of Aerosol Science* 90 (2015): 103–113, <https://doi.org/10.1016/j.jaerosci.2015.08.008>.

67. J. Ferin, “Pulmonary Retention and Clearance of Particles,” *Toxicology Letters* 72, no. 1–3 (1994): 121–125, [https://doi.org/10.1016/0378-4274\(94\)90018-3](https://doi.org/10.1016/0378-4274(94)90018-3).

68. H. R. Shamsollahi, B. Jahanbin, S. Rafieian, and M. Yunesian, “Particulates Induced Lung Inflammation and Its Consequences in the Development of Restrictive and Obstructive Lung Diseases: A Systematic Review,” *Environmental Science and Pollution Research* 28, no. 20 (2021): 25035–25050, <https://doi.org/10.1007/s11356-021-13559-5>.

## Supporting Information

Additional supporting information can be found online in the Supporting Information section. **Supporting Information 1.** Table S1: XRF detection limits for the analyzed elements. Table S2: Inhalation reference concentration (RfC) and inhalation unit risk (IUR) values used in the health risk assessment. Table S3: Mean, minimum, maximum, and standard deviation of rarely detected elements. Table S4: PMF base-run settings and error-estimation results. Figure S1: XRD pattern of a selected PM<sub>2.5</sub> sample. Figure S2: SEM micrograph and EDS elemental maps of a representative sample. Figure S3: Observed versus predicted concentration scatter plots. Figure S4: Observed versus predicted concentration time-series plots. Figure S5: Contribution of the identified sources to PM<sub>2.5</sub>. **Supporting Information 2.** Excel file EX1 provides the complete dataset of PM<sub>2.5</sub> elemental concentrations and their corresponding uncertainties for all analyzed samples.